X-ray dose reduction using additional copper filtration for abdominal digital radiography: Evaluation using signal difference-to-noise ratio

TITLE

X-ray dose reduction using additional copper filtration for abdominal digital radiography: Evaluation using signal difference-to-noise ratio

Authors

Hiroki Kawashima
Faculty of Health Sciences, Institute of Medical, Pharmaceutical and Health Sciences, Kanazawa University

Katsuhiro Ichikawa
Faculty of Health Sciences, Institute of Medical, Pharmaceutical and Health Sciences, Kanazawa University

Daisuke Nagasou
Division of Health Sciences, Graduate School of Medical Sciences, Kanazawa University

Masayuki Hattori
Division of Health Sciences, Graduate School of Medical Sciences, Kanazawa University

Corresponding Author

Hiroki Kawashima Ph.D.
Faculty of Health Sciences, Institute of Medical, Pharmaceutical and Health Sciences, Kanazawa University
E-mail: kawa3@med.kanazawa-u.ac.jp
Post-code:920-0942, 5-11-80 Kodatsuno, Kanazawa, Japan
Tel: +81-76-265-2531

Abstract

Purpose: X-ray dose reduction using additional copper filters (Cu-filters) for abdominal general radiography was indicated in a report using a simulation study. We validated the dose reduction effects using a clinical digital radiography system equipped with an indirect-type CsI detector and an automatic Cu-filter insertion function.

Methods: The image qualities were evaluated using signal difference-to-noise ratio (SDNR) for different radiation qualities with and without Cu-filters for a 20-cm acrylic phantom. Acrylic and bone equivalent material plates were used for contrast measurements. The dose reduction using Cu-filters was estimated from the ratios of the $SDNR^2$ values.

Results: For the same entrance surface dose (ESD), Cu-filters with 0.1- and 0.2-mm thicknesses increased the image quality as evaluated by $SDNR^2$ and the estimated dose reduction without degrading the image quality. For the acrylic contrast, the dose reductions with the 0.1- and 0.2-mm-thick Cu-filters were approximately 30% and 44% at 70 kV and 29% and 35% at 80 kV, respectively. For the bone contrast, the reduction rates were slightly reduced.

Conclusions: We validated the dose reduction capability of additional Cu-filters without degrading the image quality for abdominal radiography. The estimated entrance surface dose reductions of the Cu-filters were approximately 30%–40% and 20%–30% for the acrylic and bone contrasts, respectively, and effective dose reductions for acrylic were nearly half of those for ESD. At these reduced dose conditions, the current time product values needed to be increased by factors of 1.4 and 1.8 for the 0.1- and 0.2-mm-thick Cu-filters, respectively.

Keywords

Cu-filter, dose reduction, abdominal radiography, signal difference-to-noise ratio

Introduction

Recently, most of screen-film systems for X-ray general radiography have been replaced by digital radiography (DR) systems, and the usefulness for image processing and facilities in image communication of DR systems have been accepted in clinical fields [1, 2]. Especially for indirect-type flat panel detectors with phosphors of CsI and direct-type flat panel detectors using amorphous Se (aSe), their high X-ray efficiencies have contributed to reductions of radiation dose [3].

The patient absorbed dose depends not only on the amount of entrance surface dose (ESD) but also on the radiation quality. The radiation quality can be changed by selecting the X-ray tube voltage and using additional metal filters. According to a report by Martin, an additional copper filter (Cu-filter) with a thickness of 0.2 mm is sufficiently effective to reduce the ESD by 40%–50% for abdominal radiography, while maintaining the image quality as indexed by the contrast-to-noise ratio [4]. The report suggested that the dose reduction results from the removal of lower energy photons, which are absorbed in the object, and therefore, do not reach the image receptor [4]. However, their results were simulated using a spreadsheet calculation with the X-ray spectra, filters, phantom and tissue mass attenuation coefficients, and phosphor mass energy absorption coefficients. For chest radiography, the effectiveness of Cu-filters has been demonstrated using clinical indirect-type flat panel detectors [5, 6].

The disadvantages of using Cu-filters in clinical fields are an increase in the X-ray tube loads to compensate for the exposure dose decrease due to the Cu-filter and a laborious operation for inserting and removing the Cu-filter during various examinations. The former is overcome by the recent X-ray generators that are capable of routinely used tube currents more than 500 mA and higher sensitivities of DR systems [7], and the latter is solved by the automatic insertion functions mostly implemented in the recent DR systems combined with X-ray units. Therefore, the Cu-filter can be used clinically for abdominal radiography in recent times if the dose reduction effect of the

Cu-filter is validated in current clinical DR systems.

The standard abdominal radiograph needs a large exposed area, which extends from the diaphragm to the inferior pubic rami and includes the lateral abdominal wall. Since the anatomy of the abdomen is complicated, numerous structures are not clearly defined. The assessment of the bowel gas patterns and soft tissue structures is comparably important, and bones in the abdominal radiographs tend to be better visualized with dedicated bone radiographs. For the radiographic technique, tube voltages of 70-90 kV, large focal spot sizes of ~1 mm, and anti-scatter grids are used [8-10]. High resolution image processing such as edge enhancement are generally not selected because of the soft tissue depictions. The radiation dose required to obtain an adult abdominal radiograph is at least 20 times more than required to obtain an adult chest radiograph, according to several national diagnostic reference levels [11], and though it is generally performed in a supine posture, it is sometime performed with other postures (upright, decubitus, etc.). Therefore, the adequate radiation doses that reasonably achieve the depiction of abovementioned anatomies should be selected.

The purpose of this study was to validate the effectiveness of the Cu-filter through physical image quality evaluations using a DR system equipped with an indirect-type CsI detector and an automatic Cu-filter insertion function.

1. Materials and Methods

1.1 DR system and Phantom

The DR system used was an AXIOM Luminous dRF (SIEMENS, Erlangen, Germany) comprising an indirect-type CsI detector (Trixell Pixium RF4343) with a 0.148-mm pixel pitch. A standard X-ray grid of this system (ratio 15:1, density 80 lines/cm, aluminum interspace material) was also used. 0.1- and 0.2-mm-thick built-in Cu-filters could be selected for each exposure. For the image measurement, raw image data to which any additional post-processing was not applied were

used.

An acrylic phantom having a thickness of 20 cm made from 30 × 30 cm^2 slabs was used to model the X-ray absorption of an adult abdomen [12, 13] based on the standard abdominal thickness indicated in the Japanese diagnostic reference levels (Japan DRLs 2015) [14].

1.2 Radiation qualities

The tube voltages used were 70, 80, 90, and 100 kV. For 70 and 80 kV, no filter, 0.1- and 0.2-mm-thick Cu-filters are tested. The 90 and 100 kV voltages were used as high radiation qualities without using Cu-filter. For each radiation quality, we measured the half-value layer (HVL) using aluminum filters [10 × 10 cm^2 aluminum plates (type-1100, 99% purity) with nominal thicknesses of 0.5 and 1.0 mm] to obtain the effective energy. The measured HVLs and estimated effective energies are shown in Table 1. The effective energies when using Cu-filters were higher than that of 100 kV (no filter).

Table 1. HVL value and effective energy for each radiation quality

Exposure condition	HVL (mmAl)	Effective energy (keV)
70 kV	2.85	32.2
70 kV 0.1-mm Cu	4.30	38.4
70 kV 0.2-mm Cu	5.11	41.8
80kV	3.24	33.9
80 kV 0.1-mm Cu	4.84	40.7
80 kV 0.2-mm Cu	5.23	42.3
90 kV	3.60	35.4
100 kV	4.03	37.2

1.3 Exposure conditions

Figure 1 shows the geometric arrangement for image quality evaluations. The radiation field was set to 34 × 38 cm^2, and a constant ESD of 3.0 mGy at the surface of acrylic phantom was set for all radiation qualities. This ESD value was chosen based on the Japan DRLs 2015 [14]. An acrylic plate and a plate made of a bone equivalent material (4120-220 BE-H-10, Kyoto Kagaku, Kyoto, Japan) both with a 1-cm thickness and 2 × 2 cm^2 area were placed on the acrylic phantom, which were used for measuring contrasts corresponding to the soft tissues and bones included in the abdominal radiographs, which is described later. We examined another placement of the plates between two 10-cm-thick acrylics (sandwiched placement); the contrast values for the sandwiched placements were also measured.

For the ESD measurement, a 6-cm^3 general-purpose ionization chamber (Model 20X6-6; Radcal, Monrovia, CA) and an electrometer (Model 2026C; Radcal) were used. The ionization chamber was located 65 cm from the X-ray focal spot, and the acrylic phantom shown in Fig. 1 was removed when measuring the dose. We measured the exposure dose for each radiation quality with a constant tube current-time product of 10 mAs. Then, each value of ESD per unit mAs was calculated to obtain the required mAs values for constant ESD, which were combined with the backscatter factors corresponding to the radiation qualities (HVL) and the radiation field [15] and the distance factors based on the inverse square theorem.

1.4 Image measurements

In contrast to screen-film radiography, subject contrast in a digital image can be manipulated to achieve the desired contrast, and thus contrast is no longer the dominant factor for image quality. A more relevant measure of the image quality is the signal difference-to-noise ratio (SDNR), which is effective in the presence of radiation scattering objects. A digital image with a higher level of SDNR could provide inherently superior image quality [5, 16]. SDNR is calculated from the

following equation [17]:

$$SDNR = |C| \times SNR, \qquad (1)$$

where *SNR* is the signal-to-noise ratio of the phantom background (the uniformly exposed area of the acrylic phantom) and *C* is the subject contrast.

Although the SNR in Eq. (1) could simply be measured as a ratio of the background signal level, S_B to the background noise, σ_B (the standard deviation), the grid lines could cause errors in the background noise estimation. As shown in figure 2, which presents the detailed view of a region of interest in the image obtained at 70 kV without Cu-filters, the grid lines were not entirely suppressed and remained as aliased signals (periodic patterns) in the image even when the standard grid for the DR system was used. In fact, a large peak at approximately 0.4 cycles/mm in the direction perpendicular to the grid lines appeared in the noise power spectrum analyses, which were preliminarily performed. Therefore, to avoid the effect of the periodic patterns and obtain both the random and structure noise amounts, we measured the background noise using noise power spectrum (NPS) in the grid-line direction. Then, σ_B was calculated from the measured NPS using the following relationship [18],

$$\sigma_B = \sqrt{\int uNPS(u)du} \qquad (2)$$

where u is the spatial frequency in the grid-line direction. We used σ_B for the calculation of the background SNR in Eq. (1).

The contrast, *C*, was calculated from the signal levels measured on the acrylic plate, bone equivalent material plate, and background. Region of interest (ROIs) of 10 × 10 mm^2 were used to measure the average pixel value (ROI_M) on the two plates and the background between the two plates (ROI_B). The *C* value was calculated as $(ROI_M - ROI_B) / ROI_B$.

For each NPS measurement, a background area with 1024 × 1024 pixels was used for each radiation quality measurement; therefore, sixteen 256 × 256-pixel ROIs were used for the NPS calculations. For each 256 × 256-pixel ROI, after the trend removal via a fitted two-dimensional

second-order polynomial, the power spectrum was computed using a two-dimensional (2D) fast Fourier transformation. The one-dimensional NPS in the grid-line direction was obtained by averaging the directional frequency bands in the 2D NPS using the vertical axis and ±7 lines (a total of 15 lines) [19]. The resultant NPS was then calculated by averaging the NPSs of sixteen ROIs.

1.5 Dose reduction estimation

The dose reduction using the Cu-filters was estimated from the ratios of the $SDNR^2$ values with and without Cu-filters ($SDNR^2$ with Cu-filters/$SDNR^2$ without Cu-filters) for 70 kV and 80 kV based on the dose proportionality of $SDNR^2$ [5]. To validate the estimated dose reduction, the 20-cm phantom with acrylic and plate was imaged with reduced doses (mAs values) calculated from the estimated dose reduction rates for 0.1- and 0.2-mm Cu-filters, respectively, of 70 kV and 80 kV. SDNRs were measured from the obtained images using the same method as described earlier and compared with the values obtained without Cu-filters. In addition, an acrylic contrast detail phantom with a thickness of 1.5 cm (the diameters and depths of the drilled holes were each 0.5–10 mm) placed on an 18.5-cm-thick acrylic (for a total thickness of 20 cm) was imaged, without Cu-filters and with 0.2-mm Cu-filter at the same ESD and with 0.2-mm Cu-filter at the reduced dose. These images were obtained only to present the visual differences of noise amount in the three images under the same contrast.

1.6 Average organ dose and effective dose estimations

For evaluating the radiation dose in terms of patient risk, it would be desirable to measure the actual effective dose for each radiation quality. However, obtaining the effective dose is difficult because it is difficult to measure the organ doses experimentally [20]. In addition, according to the International Commission on Radiological Protection (ICRP) publication 103, the use of the effective dose for diagnostic radiography is problematic because organs and tissues receive only

partial exposure, which, in turn, results in uncertainty in organ dose estimation [21, 22]. Therefore, we chose ESD as the primal dose index.

Although the effective dose evaluation for diagnostic radiograph is problematic as mentioned above, it can be estimated using a dedicated software package based on Monte Carlo simulations, PCXMC ver. 2.0 (STUK, Helsinki, Finland). We used this software package to estimate percentage dose reduction values of the average organ dose (indicated as 'Average dose in total body' in PCXMC) and effective dose for the conditions corresponding to Figure 4 on equalized $SDNR^2$ for acrylic. In the software, “standard adult” with a height of 178.6 cm, a weight of 73.2 kg, and a trunk thickness of 20 cm was selected as the phantom type, and the incident air kerma (not ESD) values corresponding to conditions of the equalized $SDNR^2$ were entered. Since PCXMC accepted not ESD but incident air kerma, we used the incident air kerma values calculated back from ESDs using the back scatter factors. A total filtration of the X-ray tube and the collimator was set to 3.5 mm Al, as per the specifications of the DR system used.

2. Results

2.1 Contrast

Table 2 shows the results of the contrast measurement for the on-top placement of two plates, where the relative value was calculated based on the value at 70 kV without a Cu-filter. The decrease in the ratios for the Cu-filters relative to the no-filter case for acrylic was 4%–7%, while that for the bones was slightly higher (6%–11%). The high tube voltages significantly decrease the contrasts for both acrylic and bones. The contrast values for the sandwiched placement of the two plates were nearly identical to the values for the on-top placement (the relative values to the on-top placement were −1.73% ± 1.59% for acrylic and +1.65% ± 0.94% for bone). Therefore, we only used the contrast values of the on-top placement.

Table 2. Measured contrasts of acrylic and bone equivalent material plates with the on-top placement, where the relative value was calculated based on the result of a tube voltage of 70 kV without Cu-filter. The values in parentheses are relative ones to 80 kV without Cu-filter.

Radiation quality	Acrylic	Bone
70 kV	1	1
70 kV 0.1-mm Cu	0.96	0.94
70 kV 0.2-mm Cu	094	0.89
90 kV	0.73	0.64
100 kV	0.66	0.55
80 kV	0.83 (1)	0.76 (1)
80 kV 0.1-mm Cu	0.79 (0.95)	0.71 (0.93)
80 kV 0.2-mm Cu	0.77 (0.93)	0.68 (0.89)

2.2 SDNR

The $SDNR^2$ values calculated using the acrylic and bone contrasts for the same ESD are shown in Fig. 3. For both the acrylic and bone contrasts, $SDNR^2$ significantly increased when using the Cu-filters. At 70, 80, 90, and 100 kV without a Cu-filter, although the $SDNR^2$ values for the acrylic contrast were similar, the $SDNR^2$ values for the bone contrast decreased with increasing tube voltage.

2.3 Dose reductions with Cu-filters

Table 3 presents the estimated dose reduction using the Cu-filters. The percentage entrance dose reductions for the acrylic contrast were 29.2%–43.7%, whereas those for the bone contrast were 23.7%–37.7%. As shown in Fig. 4, the $SDNR^2$ values measured from the reduced dose images were nearly equal to those of the no-filter images. The dose reduction estimated from $SDNR^2$ values,

which were measured using the simple background standard deviations including the periodic patterns from grid lines, were 31.2% for acrylic contrasts at 70 kV with the 0.2-mm-thick Cu-filter, and it was significantly lower than our estimation (43.7%) using $SDNR^2$ measured by the NPS analysis in the grid-line direction.

Figure 5 shows enlarged images of a part of the contrast detail phantom for 70 kV with/without the 0.2-mm-thick Cu-filter at the same ESD (3.0 mGy) and 70 kV with the 0.2-mm-thick Cu-filter at a 40% reduced dose intending to nearly equalize SDNR to that of the image without the Cu-filter. The window conditions for the three images were adjusted based on the ROI measurements at the drilled holes and background such that the display contrasts were nearly identical. For the comparison between images with the same ESD, the image with the 0.2-mm-thick Cu-filter presented a noise-reduced image, demonstrating its better SDNR. The image at the reduced dose showed nearly identical noise to the image without Cu-filter, demonstrating the equalized SDNRs.

2.4 Average organ dose and effective dose reductions

The percentage dose reductions of average organ dose with 0.1- and 0.2-mm-thick Cu-filters for acrylic were approximately 17% and 27% at 70 kV and 16% and 22% at 80 kV, respectively. Corresponding values for the effective dose were 14% and 23% at 70 kV and 13% and 19% at 80 kV, respectively, which were somewhat lower than those of the average organ dose. Thus, the dose reductions by Cu-filters estimated using the effective dose are nearly half of those for ESD.

Table 3. Percentage entrance dose reductions with Cu-filters estimated from rates of average $SDNR^2$ values of images without/with Cu-filters.

Exposure condition	Dose reduction [%]	
	Acrylic contrast	Bone contrast
70 kV	-	-
70 kV 0.1-mm Cu	30.4	25.9
70 kV 0.2-mm Cu	43.7	37.7
80 kV	-	-
80 kV 0.1-mm Cu	29.2	23.7
80 kV 0.2-mm Cu	35.4	28.1

3. Discussion

The image contrasts of the acrylic and bone plates at the highest tube voltage of 100 kV were decreased by approximately 34% and 45%, respectively, compared with 70 kV without the Cu-filter. On the contrary, the contrast decreases of 70 kV with 0.2-mm-thick Cu-filter were significantly lower (approximately 6% and 11%, respectively), despite the higher effective energy than that with 100 kV (41.8 keV for 70 kV with 0.2–mm-thick Cu-filter, 37.2 keV for 100 kV). These results demonstrated simulation results of Martin et al., which indicated that the Cu-filter absorbed the low-energy X-ray proportion that did not contribute to imaging and simultaneously maintained the proportion that contributed to imaging [4]. Therefore, the main cause of contrast reduction was increasing the maximum energy and not increasing the effective energy in this comparison.

For the same ESD, the $SDNR^2$ values significantly increased when using Cu-filters at both 70 and 80 kV, which demonstrates the dose reduction capability of Cu-filters. The estimated percentage entrance dose reductions for the acrylic contrasts with 0.1- and 0.2-mm-thick Cu-filters were approximately 30% and 44% at 70 kV and 29% and 35% at 80 kV, respectively. For the bone

contrast, the percentage entrance dose reductions were slightly reduced (approximately 30% and 37% at 70 kV and 24% and 26% at 80 kV, respectively). The bone with higher mean atomic number has higher energy dependency of the contrast, compared with the soft tissue (acrylic), due to the higher energy dependency of the photo-electric effect. Therefore, as shown in Table 2, the bone contrast was slightly more reduced by Cu-filters compared with the acrylic contrast, which affected the percentage entrance dose reduction. Therefore, due to the equivalency between acrylic and soft-tissues [13], the use of a Cu-filter would be effective for soft-tissues and would provide slightly reduced effects for bone (i.e., spinal bones in abdominal images). In addition, our results indicate that high tube voltages of 90 and 100 kV are ineffective for dose reduction in abdominal X-ray radiography. Even though the percentage entrance dose reduction with a 0.2-mm-thick Cu-filter reported by Martin was 50% at 70–80 kV [4], our results, which were actually measured using a clinical DR system, did not reach this level and the percentages for bones were significantly reduced. The estimated dose reduction was proved by the equalized $SDNR^2$ results shown in Figs. 4 and 5. The dose reduction estimated using the $SDNR^2$ values, which was simply calculated from the background standard deviation (31.2% for the 0.2-mm-thick Cu-filter at 70 kV), was significantly lower than our percentage entrance dose reduction (43.7%) estimated using NPS analysis performed to avoid the influence of the periodic patterns from grid lines. When using the percentage value of 31.2%, it was apparent that the $SDNR^2$ values would not equalize, which indicates that the random noise components in image would not equalize. The frequency analysis we used in this study to avoid the influence of the grid lines seemed to be effective to assess the percentage entrance dose reduction using Cu-filters in the presence of a grid. However, since noise evaluation methods including the periodic patterns have not been established, further investigations with the grid line would be needed.

It has been said that filtration forces increase in the current time product (mAs); therefore, it is difficult to use clinically due to increases in X-ray tube heating. In our results, the mAs increase

factors for the 0.1- and 0.2-mm-thick Cu-filters were approximately 1.4 and 1.8, respectively, for the equalized image qualities. In the hospital where the first and second authors work, approximately 17 mAs on average is used for an adult abdomen and corresponding ESD was 1.0 mGy. The timer is approximately 34 ms for a tube current of 500 mA, which is automatically set in the mAs-control mode of the X-ray system. Therefore, the timers for the 0.1- and 0.2-mm-thick Cu-filters would need to be prolonged to 48 and 61 ms, respectively. However, these times are not too long to obtain abdominal images without motion artifacts. For the ESD of 3.0 mGy corresponding to Japan DRL, the timer was 100 ms for the 20-cm phantom, and thereby the timer would be prolonged to 140 and 180 ms, which were still smaller than recommendations (<400 ms) found in a guide line [8].

In clinical examinations, AEC systems have been routinely used. The AEC system works to approximately equalize the detector entrance dose and consequently nearly equalize the image noise. Thereby, when using the Cu-filters with AEC, it is expected that the SDNR is nearly maintained due to the AEC performance. We performed acquisitions of the 20-cm acrylic phantom with AEC at 70 kV using the DR system used in this study. As a result, the mAs values were adjusted so that the dose reductions near our results were obtained (34.0% and 46.5% for 0.1- and 0.2-mm thickness Cu-filters, respectively), which would slightly degrade SDNRs. Therefore, it appeared that the Cu-filters could be used in the routine examination using the AEC system and contribute to the ESD reduction.

The dose distributions in the depth direction are different for different radiation qualities due to their different energy absorptions. The 70 and 80 kV cases without a Cu-filter present rapid decreases from the phantom surface to deep points compared to the 70 and 80 kV cases with Cu-filters. Therefore, it is likely that the average depth-dose for the radiation quality with a Cu-filter tends to be higher than that without a Cu-filter; consequently, the image quality improves owing to the higher transmitted dose. Conversely, for conditions with the same image quality (the equalized $SDNR^2$ values in this study), the Cu-filter decreases the ESD and the transmitted dose becomes similar to that without a Cu-filter. Therefore, the average depth-dose with a Cu-filter could be reduced

compared to the condition without a Cu-filter, whereas this reduction will be less than with ESD. This point was indicated in the results of average organ dose reduction estimated using PCXMC (27% at 70 kV and 22% at 80 kV for average organ dose versus 44% at 70 kV and 35% at 80 kV for ESD, with a 0.2-mm-thick Cu-filter). Each organ dose differed depending on its depth from the surface. The organ doses close to the surface, such as liver, are more affected by the ESD difference caused by the Cu-filters, and the organ doses at deep locations such as kidney and lower spine become similar because the transmitted doses with and without a Cu-filter are nearly equalized to achieve the equalized $SDNR^2$. Therefore, it appeared that the average organ dose reductions were less than those of ESD. In addition, the tissue weighting factors of organs are multiplied to the organ doses for deriving the effective dose. As a result, affected by the tissue weighting factors (for example, a low weighting factor of liver), the effective dose reduction became a little less than the average organ dose reduction, and thus the dose reductions estimating using effective dose, which were related to risk to the patient, became approximately half of those for ESD. However, it was indicated that the effective dose reductions of 23% at 70 kV and 19% at 80 kV would be expected using the 0.2-mm-thick Cu-filter.

This study was based on one specific phantom thickness (20 cm) corresponding to a standard adult abdomen, and dose reduction estimations would be different for other thicknesses and field sizes. The dose reduction ability of Cu-filters obtained in this study needs to be confirmed by an adequate clinical study.

4. Conclusions

We validated the dose reduction capability of including Cu-filters for abdominal radiography using a DR system equipped with an indirect-type CsI detector and automatic Cu-filter insertion mechanism. The estimated entrance dose reductions for soft tissue using the 0.1- and 0.2-mm-thick Cu-filters were found to be approximately 30% and 44% at 70 kV and 29% and 35%

at 80 kV, respectively, and corresponding dose reductions estimated using the effective dose are nearly half of those for ESD. In this case, the increasing mAs factors for the 0.1- and 0.2-mm-thick Cu-filters were 1.4 and 1.8, respectively.

5. References

[1] Doi K. Diagnostic imaging over the last 50 years: research and development in medical imaging science and technology. Phys Med Biol. 2006;51:R5-27.

[2] Korner M, Weber CH, Wirth S, Pfeifer KJ, Reiser MF, Treitl M. Advances in digital radiography: physical principles and system overview. Radiographics. 2007;27:675-86.

[3] Cowen AR, Kengyelics SM, Davies AG. Solid-state, flat-panel, digital radiography detectors and their physical imaging characteristics. Clin Radiol. 2008;63:487-98.

[4] Martin C. The importance of radiation quality for optimisation in radiology. Biomed Imaging Interv J. 2007;3:e38.

[5] Samei E, Dobbins JT, 3rd, Lo JY, Tornai MP. A framework for optimising the radiographic technique in digital X-ray imaging. Radiat Prot Dosimetry. 2005;114:220-9.

[6] Hamer OW, Volk M, Zorger N, Borisch I, Buttner R, Feuerbach S, et al. Contrast-detail phantom study for x-ray spectrum optimization regarding chest radiography using a cesium iodide-amorphous silicon flat-panel detector. Invest Radiol. 2004;39:610-8.

[7] Samei E, Murphy S, Christianson O. DQE of wireless digital detectors: comparative performance with differing filtration schemes. Med Phys. 2013;40:081910.

[8] European Commission. European guidelines on quality criteria for diagnostic radiographic images. Publication EUR 16260 EN Brussels, Belgium, European Commission, 1996.

[9] James B, Kelly B. The abdominal radiograph. Ulster Med J. 2013;82:179-87.

[10] American College of Radiology. ACR-SPR practice guideline for the performance of abdominal radiography. American College of Radiology website. www.acr.org/Quality-Safety/Standards-

Guidelines/Practice-Guidelines-by-Modality/Radiography. 2015 [accessed 14.9. 15].

[11] Hart D, Hillier MC, Wall BF. National reference doses for common radiographic, fluoroscopic and dental X-ray examinations in the UK. Br J Radiol. 2009;82:1-12.

[12] Anderson JA, Wang J, Clarke GD. Choice of phantom material and test protocols to determine radiation exposure rates for fluoroscopy. Radiographics. 2000;20:1033-42.

[13] Martin C. Optimisation in general radiography. Biomed Imaging Interv J. 2007;3:e18.

[14] Japan network for research and information on medical exposures (J-RIME). Diagnostic reference levels based on latest surveys in japan -Japan DRLs 2015-, http://www.radher.jp/J-RIME/report/DRLhoukokusyoEng.pdf. 2015 [accessed 22.12.15].

[15] IAEA. Absorbed Dose Determination in Photon and Electron Beams; International Code of Practice, Report 277, IAEA, Vienna, 1983.

[16] Copple C, Robertson ID, Thrall DE, Samei E. Evaluation of two objective methods to optimize kVp and personnel exposure using a digital indirect flat panel detector and simulated veterinary patients. Vet Radiol Ultrasound. 2013;54:9-16.

[17] Aslund M, Cederstrom B, Lundqvist M, Danielsson M. Scatter rejection in multislit digital mammography. Med Phys. 2006;33:933-40.

[18] Conningham IA. Applied Linear-System Theory. In Beutel J, Kundel HL, Van Metter RL, editors. Handbook of medical imaging, volume 1, Bellingham, Wash: SPIE, 2000, p. 79-159.

[19] Samei E, Flynn MJ. An experimental comparison of detector performance for direct and indirect digital radiography systems. Med Phys. 2003;30:608-22.

[20] Dobbins JT, 3rd, Samei E, Chotas HG, Warp RJ, Baydush AH, Floyd CE, Jr., et al. Chest radiography: optimization of X-ray spectrum for cesium iodide-amorphous silicon flat-panel detector. Radiology. 2003;226:221-30.

[21] ICRP, 2007. The 2007 Recommendations of the International Commission on Radiological Protection. ICRP Publication 103. Ann. ICRP 37 (2-4).

[22] UNSCEAR. Report of the United Nations Scientific Committee on the Effects of Atomic Radiation. Sources and effects of ionizing radiation, Volume I, Annex A 2008.

Figure

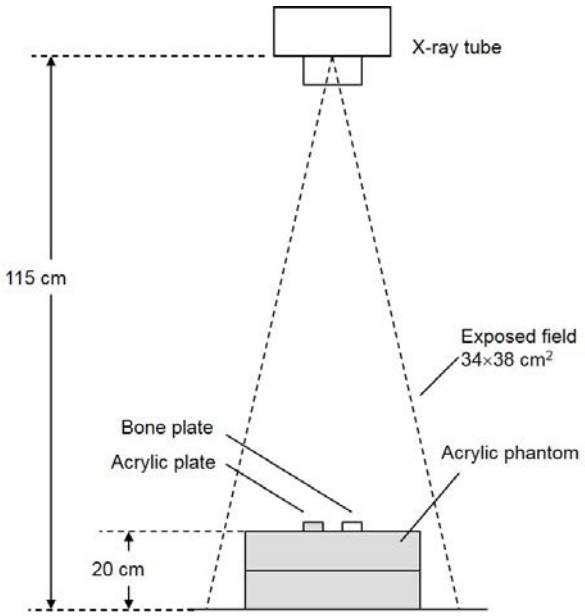

Fig. 1 Geometric arrangement for image quality measurement.

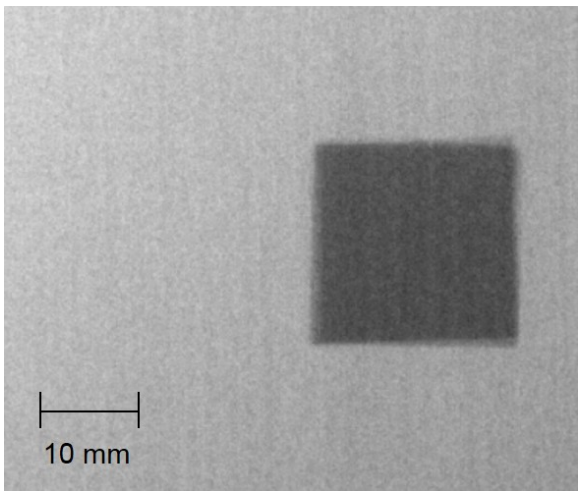

Fig.2 Detailed view of a region of interest in an image obtained at 70 kV without Cu-filters. Grid lines were not entirely suppressed and remained as aliased signals (periodic patterns) in the image.

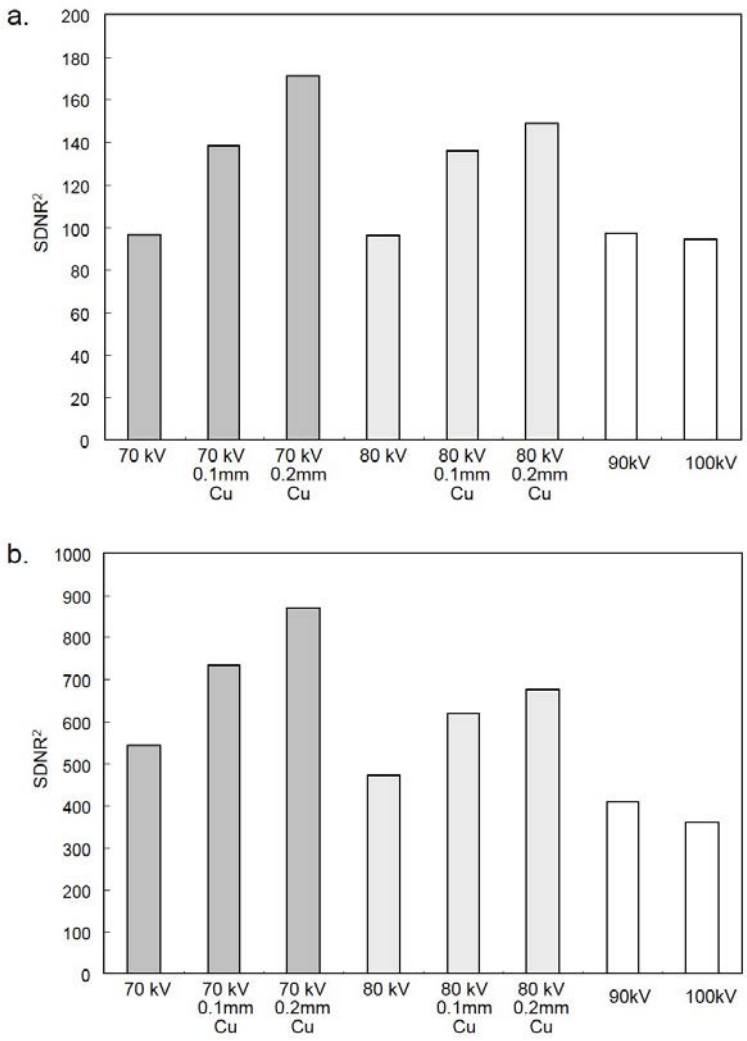

Fig. 3 $SDNR^2$ results for (a) acrylic and (b) bone with the same ESD.

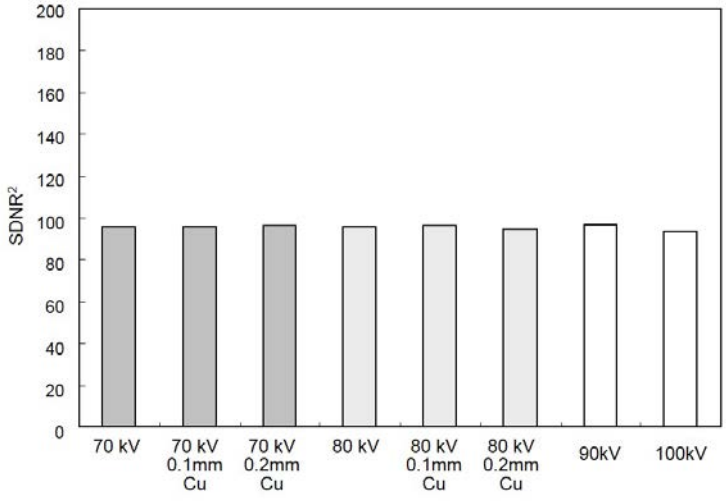

Fig. 4 $SDNR^2$ results of the dose-reduced conditions for acrylic with Cu-filters estimated

from the percentage entrance dose reduction shown in Table 3 and original conditions without a Cu-filter.

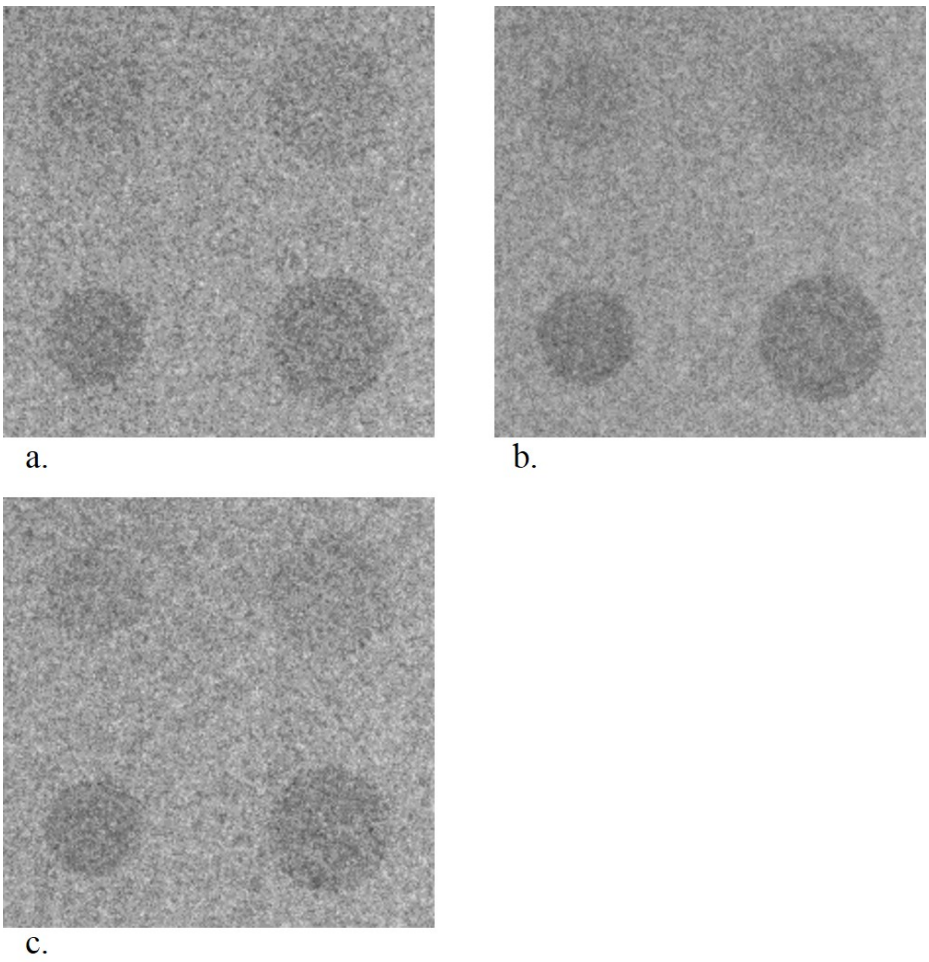

Fig. 5 Images of a part of an acrylic contrast detail phantom, which was placed on an 18.5-cm-thick acrylic contrast detail phantom (a total thickness of 20 cm). (a) 70 kV without a Cu-filter at 3mGy, (b) 70 kV with 0.2-mm-thick Cu-filter at 3 mGy, and (c) 70 kV with 0.2–mm-thick Cu-filter at a 40% reduced dose intending to nearly equalize SDNR to (a). The diameters and depths of the drilled holes were 7–9 mm and 1–2 mm, respectively. The window conditions for the three images were adjusted such that the display contrasts became almost identical.